

A LEAST SQUARES PROBLEM IN GAMMA RAY TRANSMISSION TOMOGRAPHY

*Carlos C. Dantas¹, Bruna G. M. Araújo¹, Valdemir A. dos Santos²,
Christine L. L. Finkler², Eric F. de Oliveira³, Silvio B. Melo³, M. Graça dos Santos³*

¹ Departamento de Energia Nuclear DEN - Universidade Federal de Pernambuco UFPE
Av. Professor Luiz Freire 1000, CDU; 50740-540 Recife – PE. ccd@ufpe.br

² Departamento de Química - Universidade Católica de Pernambuco
Rua do Príncipe 526, Boa Vista, 50050-410, Recife – PE. vas@unicap.br

³ Centro de Informática - Universidade Federal de Pernambuco
Recife – PE. sbm@cin.br

Abstract – The results in single beam gamma transmission tomography are presented by an image processing based on the Algebraic Reconstruction Technique - ART. The mathematical reconstruction was carried out by Bezier triangles with Bernstein polynomials, and also by spline functions, and as a matter of comparison the Filtered Backprojection - FBP method was used. The image processing reconstructs the FCC (fluidized catalytic cracking) catalyst density distribution in an experimental riser. Typical problems are characterized as reconstruction models involve the inverse problem, basis function and solution of linear system of equations. A least squares estimator is required for the numerical solution, the model parameters are evaluated, and a comparison with literature values is carried out.

Keywords: Mathematical reconstruction, Catalyst density, Single beam tomography.

1. INTRODUCTION

Computed Tomography in medical application is a quite well established method and from it industrial tomography has imported important developments like new scintillation detector types and shapes and computational algorithms. In comparison, in industrial tomography does not exist an attenuation coefficient database, nor is tomographic equipment commercially available, but on the other hand in several applications, it has a huge stain tube to penetrate that absorbs much of the whole radiation intensity and brings lots of noise to the detection and transmission measurements. Practically each research group develops its own tomographic systems so a broad variety of geometry arrangements involving parameter configurations can be found, as an example, spatial resolution of system is mainly limited by the size of the source and the detector elements, from an arc with 64 detectors, and even more sophisticated

arrangement with an arc of 360 detectors, are also described, along with single beam tomography and its parameters as discussed by S. B. Melo et al [1]. Though gamma tomography proved to be highly successful for this application the remaining problems to be solved in the future are the improvement of spatial resolution and an increase of accuracy in the reconstructed absolute mass attenuation coefficient values which may be achieved by iterative image reconstruction algorithms.

Several models to describe gamma transmission measurements are used to uncertainty evaluation. The tube wall effects are estimated in many experimental set ups, and their strong influence requires a model that takes into account the geometry of the tube (for instance [2]). Then tube thickness d was modelled as a function $d = f(Re, R)$ of the external and internal radii. The equation form that relates intensity to attenuation coefficient, used for experimental measurement calculation, is thought also as a being a possible source of error as given by C. C. Dantas et al [3]. Certainly it should be included a literature much poor in physical and mathematical fundaments as well structured subjects in literature reviews and books, are not easy to find on industrial gamma tomography. In order to fill the gap, a recent IAEA report, 2008, [4], should be mentioned that is surely a significant contribution.

The Filtered Back Projection (FBP) the well-known analytical method, is implemented in Matlab software using fast Fourier and the Radon transformation. For comparison it is used several times in this work, but in general industrial applications FBP is not adequate, and ART algorithms whose characteristics (are also described in [4]), were developed in order to carry out mathematical reconstruction. Several alternatives and refinements of the ART are considered, in this work the focus is on the system of linear equations formulated by computational algorithm and the least squares solution.

An important part of CT that needs particular attention is the estimation of error in the reconstructed image. The total error combines noise measurements and reconstruction algorithm errors and is therefore hard to estimate without Monte Carlo simulations. However, new techniques such as boot-strap techniques allow estimating error without numerous simulations. This technique can also be used to optimize the design of a CT system (as it is given in [4]).

2. EXPERIMENTAL AND METHODS

2.1. Experimental Setup

A tomographic system of single source–detector pair with stainless steel tubes of 0.154 m internal diameter follows the geometry for riser irradiation. A ^{137}Cs radioactive source ($3.7 \cdot 10^8$ Bq) and NaI(Tl) scintillation detector of (51x 51). 10^{-3} m crystal size coupled to a multichannel analyzer and Genie-software from Camberra, were installed.

Source and detector collimators of cylindrical aperture of $2 \cdot 10^{-3}$ m, $5.5 \cdot 10^{-3}$ m, $10 \cdot 10^{-3}$ m and $20 \cdot 10^{-3}$ m were used. The gamma ray transmission measurements were carried out by the 0.662 MeV photopeak. Nominally the gamma detection system has a time constant of 0.5 microsecond pulse pair resolution, nevertheless at gamma intensity measurements on the hundred kcps interval, certainly perturbation will occurs. In the range of 2 to 50 kcps spectrum broadening and peak shifting are kept under control and the linear scale of the output signal works properly.

The transmission measurement by scanning is taken along the x-axis in a coordinate system where the origin coincides with geometrical riser center. To scan the riser and generate the gamma transmission measurements matrix, A experimental configuration given by M. Azzi, P. Tulier, J.R. Bernard, L. Garnero [5], is adopted in this work.

2.2 Mathematical Reconstruction

In transmission tomography, beams of gamma radiation are passed through the equipment or section of a tube being scanned from various positions and at various angles. Each beam is detected on the equipment opposite side from the beam source, and the measured intensity I is compared to the incident intensity I_0 . If the measured attenuation of the object g , is defined as $g = \ln(I_0/I)$, then g is given by the linear transformation:

$$g = \int_L \mu(x, y) dl \quad (1)$$

where $\mu(x, y)$ is the linear attenuation coefficient of the object at the point (x, y) and L is the gamma ray path length.

To reconstruct an image and produce a graphical representation of the distribution of the process parameters it is necessary to limit the spatial resolution and define a function $\mu(x, y)$. This is an array of pixels in which each the linear attenuation coefficient is assumed to be constant. The ray sum for each ray j is then expressed by the following summation:

$$p_j = \sum_{i=1}^N w_{ji} \mu_i \quad (2)$$

where w_{ji} is the contribution to ray sum j from pixel i , μ_i is the attenuation coefficient of the pixel i and N is the number of pixels. The terms w_{ji} constitute the elements of the weight matrix W . According to the defined $\mu(x, y)$ function the number of measurements can be higher, that is, for r measurements $j = 1, \dots, r$ and $i = 1, \dots, n$ coefficients, the linear system of equations

$$W\mu = p \quad (3)$$

Will have a rectangular weight matrix with $r > n$. The solution of the least squares problem, to find the vector of coefficients μ , will minimize the norm of the residuals via normal equations. Such a solution is unique if W has a full rank.

In industrial tomography the number of measurements and the number of angles to scan the flow in a tube are limited by temporal resolution requirements. The density distribution function $\rho(x, y)$ is defined M. Azzi, P. Tulier, J.R. Bernard, L. Garnero [5], in a “natural pixel decomposition” and due to the choice of the basis function, the corresponding to W matrix in (3), would be a singular matrix. In this case the least squares method has to implement a pseudo inverse of W , and the two main algorithms to search the solution are: QR factorization and singular value decomposition SDV, as it is given by L. N. Trefethen, D. Bau III [6].

Image processing takes experimental data to define the density function $\rho(x, y)$ distribution over a tube cross section that is the basis function in a given vectorial space. The function distribution is formulated as a system of equations whose solution is an inverse problem that can require a least squares method. The non-parametric Bézier triangle is a patch of a polynomial surface, in which each variable takes barycentric coordinates with respect to a given triangle in the domain. These barycentric coordinates are arguments for the Bernstein basis, which become weights for the weighted average of the density values associated with the intersections of the gamma rays. More precisely, it can be written:

$$D(\mathbf{u}) = \sum_{|\mathbf{i}|=n} B_{\mathbf{i}}^n(\mathbf{u}) b_{\mathbf{i}} \quad (4)$$

$D(\mathbf{u})$ is the proposed density function, where $\mathbf{u} = (u, v, w)$, with $u + v + w = 1$ the barycentric coordinates of the point for which the density value is required, \mathbf{i} is a triple-index-value ijk , used to identify each intersection point and its density value, $b_{\mathbf{i}}$. In the formula, $|\mathbf{i}| = n$ means that $i + j + k = n$.

2.3 Least Squares Problem

Here it is proposed to estimate the control densities through an application of the least squares method to the function defined in the Eq. (4). We suggest that the average

of the control densities along a gamma ray trajectory is a good estimate for the actual density value from the experiments. It is not difficult to realize that the bigger the number of trajectories, the better the estimation. In barycentric coordinates, the points in a given gamma ray trajectory can be characterized as those in which one of the coordinates is a fixed positive number, less than or equal to 1. According to our choices for the triangle configuration, one such number is always of the type $i/(m-1)$ for some i in $\{0, 1, \dots, m-1\}$, where m is the number of trajectories in each edge of the triangle that circumscribes a riser's section.

We may establish that $\delta u, i$, $\delta v, j$ and $\delta w, k$ are the acquired experimental density values associated with the trajectories in which $u = i/(m-1)$, $v = j/(m-1)$ and $w = k/(m-1)$, respectively. Let i/m be the triplet $(i/(m-1), j/(m-1), k/(m-1))$. In the trajectory where $u = i_0/(m-1)$ for some i_0 , we may say that the average density of the approximating function from (4) ideally should be equal to the corresponding acquired experimental density:

$$\frac{1}{m-i_0} \sum_{|i|=m-1} D(i/m) = \delta_{u,i_0} \quad (5)$$

Substituting (1) in this equation:

$$\frac{1}{m-i_0} \sum_{|i|=m-1} \sum_{|j|=n} b_j B_j^n(i/m) = \delta_{u,i_0}$$

After rearranging it:

$$\sum_{|j|=n} b_j \left(\frac{1}{m-i_0} \sum_{|i|=m-1} B_j^n(i/m) \right) = \delta_{u,i_0} \quad (6)$$

similarly, for the trajectories where $v = j_0/(m-1)$ for some j_0 in $\{0, 1, \dots, m-1\}$ and $w = k_0/(m-1)$ for some k_0 in $\{0, 1, \dots, m-1\}$, we obtain:

$$\sum_{|j|=n} b_j \left(\frac{1}{m-j_0} \sum_{|i|=m-1} B_j^n(i/m) \right) = \delta_{v,j_0} \quad (7)$$

And

$$\sum_{|j|=n} b_j \left(\frac{1}{m-k_0} \sum_{|i|=m-1} B_j^n(i/m) \right) = \delta_{w,k_0} \quad (8)$$

These are the $3m$ rows of the overdetermined system $Ax = b$, where x contains the unknowns b_i . The least squares problem is set by the normal equations: $A^T Ax = A^T b$. The symmetric coefficient matrix of this linear system of equations possesses $(n+1)(n+2)/2$ rows and columns. Typically, when

$$n \leq \frac{\sqrt{24m+1}-3}{2} \quad (9)$$

the least squares problem will return a unique solution.

3. RESULTS

By approximate density over the tube cross section the discretization algorithm leads to a system of linear equations. As the number of measurements is constant an overdetermined system is formulated as in Equation (3). Trying to improve the reconstructed image quality, experiments with alternatives weight matrix formulation and simulations to optimize experimental conditions, also produces underdetermined systems. In computational algorithm is included Matlab built in functions to calculate the LS solution. Some of these functions automatically apply algorithms as LU, QR for both over and underdetermined systems. The Experiments with the reconstruction of the catalyst density in the riser are presented (for instance in [1], [2] and [3]), by means of an ART developed algorithm and using FBP as a matter of comparison. In Fig. 1 the reconstruction of an aluminium half-moon is given using developed algorithm and a least squares method.

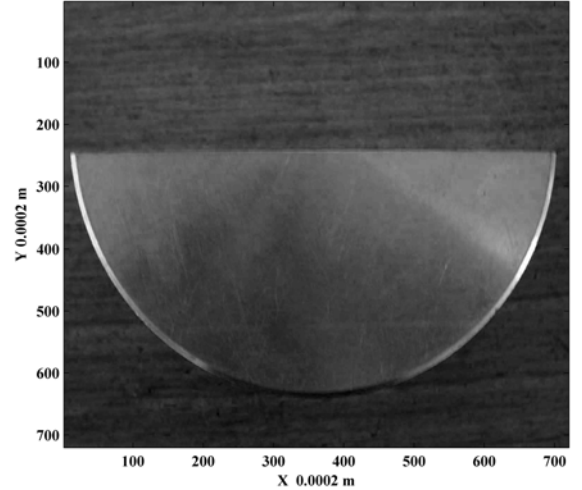


Fig. 1. Reconstructed aluminium half-moon with a photo input data.

The photo input data give a reference for errors evaluation in comparison with transmission measurements input data. A calibration of input data for the experimental measurements is carried out (as given in [7]). The initial input data were photos image of high quality as a 600 ppi (pixels per inch) photo is qualified. The photos of aluminum pieces with form, dimension and density known are shown on 20 400 ppi. photo image, that occupies 4 megabytes of memory which is a relatively big matrix that can increase computational time. From such a big matrix input data is the reconstructed image shown in Fig. 2.

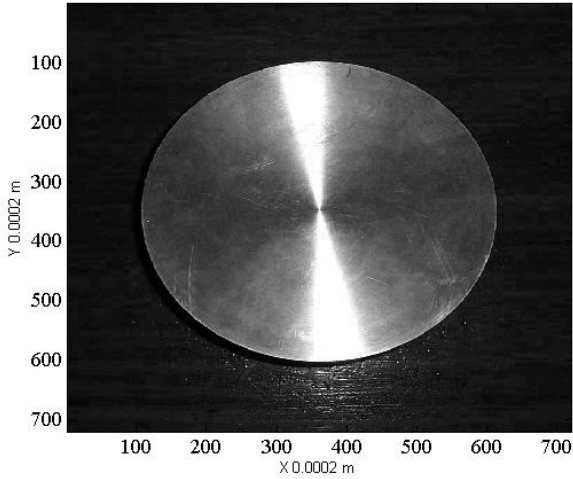


Fig. 2. Reconstructed aluminium full-moon with a photo input data.

Then, the matrix size was optimized keeping a quite high resolution 783 ppi but having only 0.15 megabyte which allows rapid computation and plenty utilization of Matlab functions to image analysis procedure. With optimized matrix size the FBP reconstruction was carried out the image quality was evaluated by RMSE and relative values on a calibration interval. The optimized input data matrix can be seen in Fig 3, and reconstructed full-moon in Fig 4.

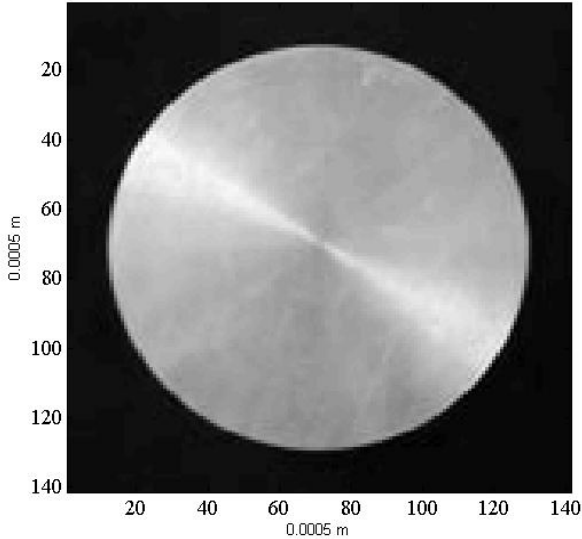


Fig. 3. Original photo of aluminium full-moon.

The image contrast seems to improve slightly from Fig 2 to Fig 4, but in the data matrix a significant different image background is obtained. By means of the optimized input data having a well defined image background, original data photo in Fig 3 and the reconstructed image in Fig 4, were evaluated, by comparing RMSE values. That is the quality of imaging reconstruction was quantified and a $(96 \pm 2) \%$ value is obtained.

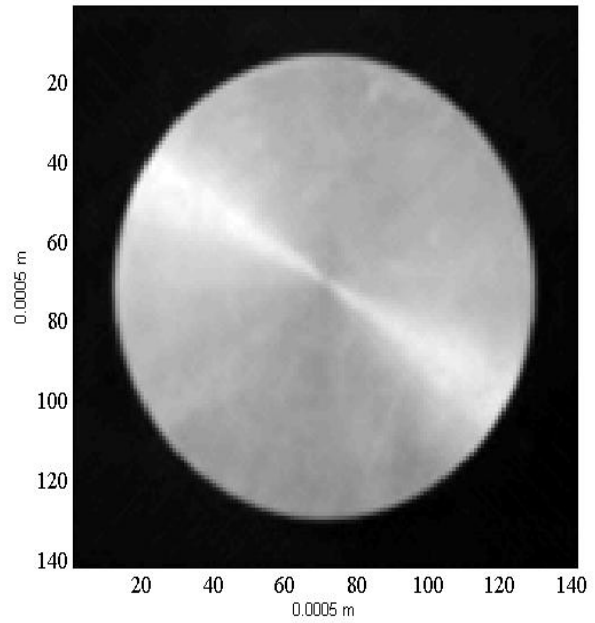


Fig. 4. Reconstructed aluminium full-moon with optimized input data.

The spatial distribution was estimated by positioning the piece inside steel tube, the experimental riser, and taken both center as coincident with the origin of coordinate system, then comparing input in Fig 3 and reconstructed image in Fig 4. The aluminium full-moon, given in Fig 3 and Fig 4, is in both figures symmetrically placed as it can be observed. The aluminium piece has a 0.060 m diameter, measured with a digital ruler, as a calibration of the density distribution for image reconstruction, the following measurements of horizontal and vertical diameters were carried out on matrix data, by Matlab functions, and an uncertainty of $(0.060 \pm 0.003) \text{ m}$ was determined .

The photos of the aluminum pieces were taken inside experimental riser, in the tomographic equipment, the measurements of the full-moon dimension, symmetry and centralized position evaluations, can be observed in the reconstruction given in Fig 5.

The image reconstructions by the FBP method are given from Fig1 to Fig 5, that are experiments with photo input data of aluminium pieces. A number of 180 projections were used and the quality of the reconstruction was evaluated by means of RMSE values. To compare with FBP the reconstruction by means of an algebraic method was carried out. An algorithm of ART kind was developed in Matlab, and the solution of the linear system of equations as it is given in Equation 3 was analysed.

The used Matlab functions includes several known algorithms: lsqr, linsolve, backslash (\), LU, QR, and mldivide. And a routine was adapted to calculate the solutions by a regularization technique. The algorithm performance for the solutions of the linear system of equations was evaluated by the number of projections and the quality of the reconstruction according to RMSE values.

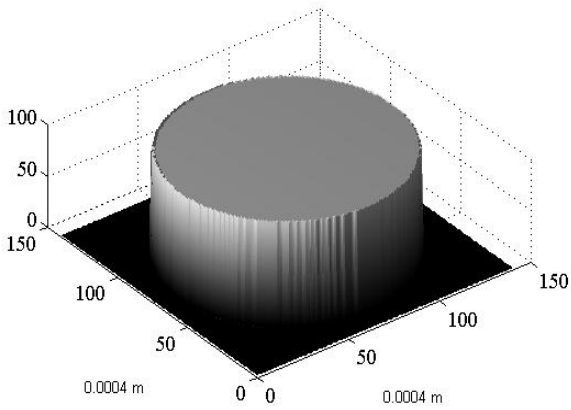


Fig. 5. Image reconstruction shown dimension and symmetry of the aluminium full-moon.

In Fig. 6 is given an image reconstructed by the ART method, with the Matlab linsolve algorithm and using 32 projections.

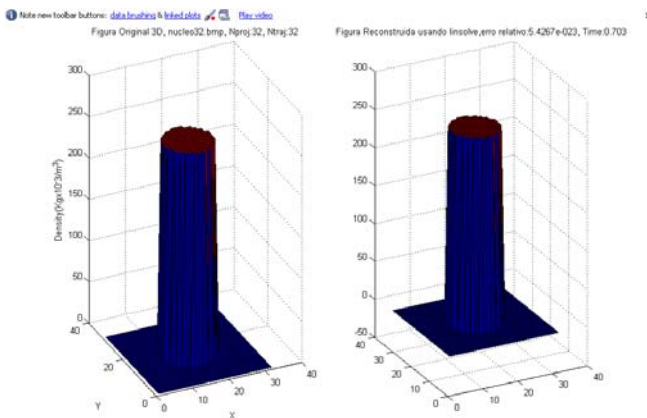


Fig. 6. Simulated on the left side and reconstructed Image on the right side.

The generated large matrixes increases ill-conditioned problems and often exceed computational memory. In this case sparse matrix implementation helps and LS solution is carried out by means of the built in functions as $x = A \setminus b$ and the lsqr instruction. An evaluation of image reconstruction corruption due to a non-unique solution calculation is studied. Analysing the weighted matrix according to full rank, condition number and the obtained residuals; such analysis is compared with parameters estimate and each associated solution of the LS problem with a formulated singular weight matrix shows a better computational stability with a regularization technique.

In Fig 7 is given the algorithm evaluation in the ART reconstruction method. The Alg1 to Alg7 are denoting the lsqr, linsolve, backslash (\setminus), LU, QR, mldivide and Tikhonov regularization, respectively.

They are Matlab functions plus a Tikhonov regularization implementation.

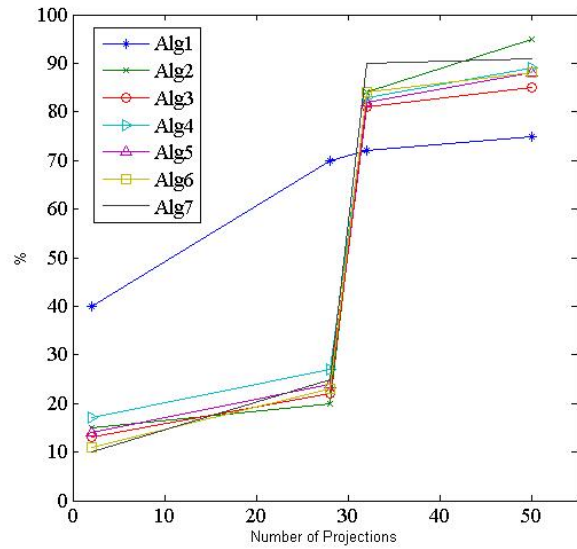


Fig. 7. The quality of reconstruction as a function of number of projections for several algorithms.

As the aim of algebraic algorithms is use few projections in opposition to FBP method, a very low number of projections were investigated. At 2 and 28 projections the performance were investigated in an undetermined system. The lsqr function - Alg1, shows a 70 percent reconstruction for 28 projections, and no significant improvement up to 50 projections. In the undetermined system all other algorithms are of low performance that improves suddenly at 32 projections, as expected, for a determined system with a square weight matrix. The algorithms show equivalent performance as the number of projections increase up to 50 projections solving a overdetermined system. In table 1, are listed the Euclidean L_2 norm of $(Ax - b)$ for three conditions of the linear system of equations.

Table 1. $L_2(Ax - b)$ values for the algorithms

Algorithm	($m < n$)	($m = n$)	($m > n$)
LSQR	0.397	0.016	0.001
linsolve	17.2	6.5e-04	0.002
(\setminus)	14.9	5.7e-05	0.002
LU	146	1.6e-05	0.002
Tikhonov	149	9.9e-05	0.002
QR	190	4.7e-04	0.002
mldivide	149	5.7e-06	0.002

The algorithms and conditions of the system of equations are for the A matrix (m, n) in Table 1, as it is formulated in the least squares problem which solutions are evaluated by the L_2 norm of $(Ax - b)$. Comparing the Table 1 and fig. 7 for the lsqr solution, as an example, this algorithm shows the best results for the A ($m < n$) case, and the worst for the two others.

All the tests are of ideal reconstruction carried out by the ART method algorithm. Experiments with noisy data are not at all satisfactory for any A ($m < n$) case and much poor reconstruction was in general obtained. For noisy data the approach given by Samuli Siltanen [8], to the inverse problem, as deblurring is to find a sharp photograph from blurry image proved to be quite adequate. A sequence of methods are proposed and Matlab routines are available, to investigate the solution of the matrix equation $b = Ax + \varepsilon$, with ε as a random vector. The experiments were carried out introducing several levels of noise in the image processing data and according to [8], restricted to white Gaussian noise. In Table 2. are given L_2 values for the solutions at a noise level $\sigma = 0.02$ for one and two-dimensional deconvolution.

Table 2. The L_2 ($Ax - b$) values at noise level $\sigma = 0.02$

Dimension	($m < n$)	($m = n$)	($m > n$)
One	0.40	0.07	0.13
Two	0.55	0.07	0.32

Dimension of the constructed measurement matrix and the noise level $\sigma=2$ in Table 2, are provided by routines that use the normal random randn-function with a defined level factor. The dimensional convolution takes the build in Matlab function convmtx for discrete vectors. Experiments with noise levels from $\sigma = 0.001$ to $\sigma = 0.90$ shown a tendency that follows the data trend in Table 2, for higher noise levels some blurry image data are unexpected results.

The non-unique solution problem required further experiments on the sparse matrix implementation exploring Matlab possibilities. Results are improved by computing the non-negative least-squares solution and by the non unique total least squares. Special structure of the weight matrix can be exploited for efficient cost function and first derivative computation, using total least squares. Based in a consistent theoretical and computational frame work, as described by (I. Markovskya and S. Van Huffelb, [9]), the method also produces the most promising results. To show the results reconstructed image are evaluated by means of comparison with original data according to RMSE values.

4. CONCLUSIONS

The developed algorithm using a basis function and discretization procedure that generates an overdetermined system of equations whose solution is carried out by least squares method proved to be efficient. In case the experiment produces a singular weight matrix the algorithm with a regularization operator shows a better performance due to numerical stability. Implemented Tikhonov methods show improvement for experiments with noisy data. At a

higher noise level the Regular Total Least Squares method might provide better results for the inverse problem as far the actual investigation is considered. Future experiments will include a wavelet basis that takes advantage of the density distribution allowing an optimized image reconstruction. A study of the image reconstruction models by means of Monte Carlo simulation in order to evaluate errors might be a road towards uncertainty estimation.

ACKNOWLEDGMENTS

The financial support of CNPq and the scholarships are greatly appreciated. The authors wish to thank Dr. Waldir P. Martignoni, Cenpes/Petrobras, for suggestions and Assistance.

REFERENCES

- [1] S. B. Melo, C. C. Dantas, E. A. O. Lima, F. P. M. Simões, E. F de Oliveira, V. A. dos Santos, Reconstruction of radial Catalyst concentration distribution in an experimental type FCC riser, *Metrology and Measurement Systems.*, Vol. XIII, 2007, p.137 – 148.
- [2] C. C. Dantas, S. B. Melo, E. F de Oliveira, F. P. M. Simões; M. G dos Santos, V.A. dos Santos, Measurement of density distribution of a cracking catalyst in experimental riser with a sampling procedure for gamma ray tomography. *Nuclear Instruments and Methods in Physics Research B, Amsterdam*, 266, 841-848, 2008.
- [3] C. C. Dantas, S. B. Melo, V.A. dos Santos, E. F. de Oliveira, F.P.M. Simões, M.G. dos Santos, A.R de Aquino, A Study of Uncertainty Evaluation In Transmission Measurement In Gamma Ray Tomography, *12th IMEKO TC1 & TC7 Joint Symposium on Man Science & Measurement*, September, 3 – 5, 2008, Annecy, France
- [4] Industrial Process Gamma Tomography, Final report of a coordinated research project 2003–2007, *IAEA – International Atomic Energy Agency*, 2008.
- [5] M. Azzi, P. Tulier, J.R. Bernard, L. Garnero, Mapping solid concentration in a circular fluid bed using gammametry, *Powder Technology*, 67, 27-36, 1991.
- [6] L. N. Trefethen, D. Bau III, Numerical Linear Algebra, *SIAM, Philadelphia* 1997 .
- [7] L. F. S. Cadiz, A. Rodrigues, E. F. Oliveira, C. C. Dantas, S. B.Melo, A Precise Image Reconstruction Procedure, “in press” *INAC2009 – International Nuclear Atlantic Conference, Sep27 - Oct 2, Rio de Janeiro, Brazil*, 2009.
- [8] Siltanen S., MAT-52506, Inverse Problems, available at web site, *InvProbSamuliluentomonistep6.pdf*, September, 2008
- [9] I. Markovskya, S. Van Huffelb, Overview of total least-squares methods, *Signal Processing* 87, 2283–2302, 2007.